Turkish Journal of Earth Sciences

http://journals.tubitak.gov.tr/earth/

Research Article

Turkish J Earth Sci
(2020) 29: 617-628
© TÜBİTAK
doi:10.3906/yer-1910-7

Zircon U-Pb age and Hf isotopic composition of the Carboniferous Gönen granitoid in the western Sakarya Zone of Turkey

Fırat ŞENGÜN[1,*], **Osman Ersin KORALAY**[2], **Magnus KRISTOFFERSEN**[3]

[1]Department of Mining and Mineral Extraction, Çan Vocational College, Çanakkale Onsekiz Mart University, Çanakkale, Turkey
[2]Department of Geological Engineering, Dokuz Eylül University, Tinaztepe Campus, İzmir, Turkey
[3]Department of Geosciences, University of Oslo, Oslo, Norway

Received: 09.10.2019 • **Accepted/Published Online:** 30.01.2020 • **Final Version:** 05.05.2020

Abstract: The Gönen granitoid is exposed in the western Sakarya Zone and is overlain unconformably by a Jurassic succession. The medium to coarse-grained Gönen granitoid has mineral assemblage of K-feldspar, plagioclase, quartz, muscovite, and biotite. Accessory phases are apatite and zircon. In this study, zircon U-Pb age is combined with Lu-Hf isotopes, which are presented to reveal the magma source and possible petrogenetic processes that took place during the formation of the parental magma for the Gönen granitoid. U-Pb dating of magmatic zircons yielded a concordia age of 336.3 ± 2.9 Ma referring to the early Carboniferous crystallization age of the Gönen granitoid. Magmatic zircons have negative $\varepsilon_{Hf}(t)$ values (–3.2 to –8.3), indicating that the granitoid magma was derived from the recycling of ancient crustal materials. T_{DM} model ages vary in the range of 1489–1811 Ma, indicating that the crustal material involved during the early Carboniferous partial melting could be extracted from the mantle or added to the basement of the Sakarya Zone in the Mesoproterozoic/Paleoproterozoic times. Geochronological and Lu-Hf findings point to a collisional setting rather than ongoing subduction during the formation of the early Carboniferous Gönen granitoid.

Key words: U-Pb zircon dating, Hf isotopes, Carboniferous Gönen granitoid, Sakarya Zone, NW Turkey

1. Introduction

Granites are principally produced by the partial melting of crustal rocks and are crucial components of continental regions and therefore include important information about the nature of ancient continental crust, tectonic and petrogenetic processes occurring during continental growth, mantle–crust interaction, and contemporaneous ore deposits in distinct tectonic settings (e.g., Hawkesworth and Kemp, 2006; Kemp et al., 2007; Gill, 2010; Brown, 2013; Lu et al., 2017). Granitic rocks display great compositional differences based on the variation in their mineralogical compositions (Pitcher, 1997; Clemens and Steven, 2012; Brown, 2013; Gao et al., 2017). Therefore, classification, magma sources, the mechanism of crust–mantle interactions, and tectonic settings are among the most controversial issues for granite petrology. The U-Pb-Hf isotopic characteristics of zircon, occurring as an accessory phase in granitic rocks, can supply useful contributions to the solution of these conflicting issues. Moreover, combining U-Pb with Lu-Hf isotope studies allows us to examine crust formation, magma sources, and juvenile-reworked crustal fragments (Condie et al., 2005; Zeh et al., 2013; Block et al., 2016; Lu et al., 2017).

The Gönen granitoid is one of numerous Variscan granitic intrusions exposed in the Sakarya Zone. The present study addresses a combined study of geochronological and Hf isotopic data encoded in zircons from the Gönen granitoid. The purpose of this paper is to determine crystallization age and source region characteristics during partial melting.

2. Geological setting

The Sakarya Zone is a tectonic unit expanding in the E-W direction along the north of Turkey from the Biga Peninsula in the west to the Eastern Pontides in the east (Figure 1a). The Sakarya Zone has a compound pre-Jurassic basement including continental and oceanic units with three distinct rock facies: i) amphibolite-granulite-facies metamorphic rocks of the Kazdağ, Uludağ, Kurtoğlu, and Pulur Massifs with metamorphism ages of 310–334 Ma (Carboniferous) (Topuz and Altherr, 2004; Okay et al., 2006; Topuz et al., 2007; Erdoğan et al., 2013); ii) Devonian to Permian granitoids and acidic volcanic rocks (Okay et al., 1996, 2006; Topuz et al., 2004, 2010; Dokuz, 2011; Aysal et al., 2012a, 2012b; Sunal, 2012; Karslı et al.,

* Correspondence: firatsengun@comu.edu.tr

2016; Kaygusuz et al., 2016; Dokuz et al., 2017; Şengün and Koralay, 2017); and iii) the Permo-Triassic Karakaya Complex composed of the lower Karakaya unit and upper Karakaya unit (Okay and Göncüoğlu, 2004). Greenschist-facies metamorphic rocks with Late Triassic eclogites and blueschists characterize the lower Karakaya unit. However, the upper Karakaya unit, which tectonically overlies the low-grade metamorphic rocks of the lower unit, is mainly dominated by highly deformed clastic and volcanic rocks comprising Carboniferous-Permian limestone blocks and Permian to Late Triassic radiolarian cherts. Lower Jurassic sedimentary successions and volcanic rocks unconformably cover all the rocks of the pre-Jurassic basement in the Sakarya Zone (Figure 1b).

The Gönen granitoid is a 1-km-long and 750-m-wide stock that trends NE-SW in the village of Hafız Hüseyinbey (Figure 2). The Gönen granitoid has medium to coarse-grained texture, brown to yellowish color, and highly weathered outcrops in the field, and it appears to be one of the members of the numerous postcollisional Variscan granitoids in the Sakarya Zone (Figure 3a; Topuz et al., 2007; Dokuz, 2011; Ustaömer PA et al., 2012; Ustaömer T et al., 2013). Similar to the other pre-Jurassic rocks in the Sakarya Zone, it is unconformably overlain by conglomerate, sandstone, siltstone, and claystone intercalations of the Early Jurassic Bayırköy Formation (Figure 3b). Based on the fossil fauna reported from red nodular ammonitico rosso limestones intercalated within these clastic rocks, the age of the Bayırköy Formation is given as Hettangian-Early Pliensbachian (Okay et al., 1991).

3. Analytical techniques

One sample (1805; 35S 0544696N-4447370E) was selected from the Gönen granitoid for zircon U-Pb-Hf isotopic analyses. The sample location is given in Figure 2.

Zircons were separated from a granitoid sample (1805) weighing 6 to 8 kg by traditional techniques of crushing, magnetic, and heavy-liquid separation. Clean and inclusion-free zircon grains were separated under a binocular microscope. Extracted zircons were embedded in epoxy and polished. Zircon grains were imaged by cathodoluminescence (CL) with a Hitachi S3400N scanning electron microscope (SEM) at the Earth Sciences Department of Gothenburg University (Sweden) to determine the external morphology and internal structure.

U-Pb and Lu-Hf isotopic analyses of zircon crystals were completed by ICP-MS with a Nu Plasma HR multicollector combined with a Cetac LSX-213 G2 laser microprobe (with HelEx cell) at the Geosciences Department of Oslo University. The laser beam was set to 10-Hz repetition rate with a spot size of 40 µm and beam energy density of 0.07 J/cm^2. Each zircon analysis included background measurement of 30 s and was followed by ablation of 60 s. Analysis series are composed of blocks of 15 unknowns, bracketed by 4 analyses of zircon standards. Zircon standards used for calibration are A382 (1877 ± 2 Ma; Lauri et al., 2011), 91500 (1060 ± 1 Ma; Wiedanback et al., 1995), and GJ (609 ± 1 Ma; Jackson et al., 2004). Correction and background subtraction were done using an in-house Microsoft Excel interactive spreadsheet program. All concordance ages were estimated using Isoplot (Ludwig, 2012), version 4.12. More details about the analytical procedure of the zircon U-Pb dating were given by Andersen et al. (2009).

Hf isotopic analyses were performed on the same spots as all U-Pb dated zircon grains. The analytical protocols for Lu-Hf analyses described by Elburg et al. (2013) were used. Conditions of ablation were set as 50-µm beam diameter and pulse frequency of 5 Hz. LV-11 zircon (Heinonen et al., 2010) and Mud Tank zircon (Woodhead and Hergt, 2005) were used as Lu-Hf standards. Mud Tank zircon ($^{176}Hf/^{177}Hf$ = 0.282505 ± 4) gave $^{176}Hf/^{177}Hf$ = 0.282533 ± 30 (2 SD; n = 102) and reference zircon LV-11 ($^{176}Hf/^{177}Hf$ = 0.282830 ± 28) yielded $^{176}Hf/^{177}Hf$ = 0.282825 ± 34 (2 SD; n = 120) during analyses of zircons. The decay constant of 1.867×10^{-11} $year^{-1}$ for ^{176}Lu as well as $^{176}Lu/^{177}Hf$ = 0.0336 and $^{176}Hf/^{177}Hf$ = 0.282795 values of present-day chondritic were used to estimate all ε_{Hf} values (Söderlund et al., 2004; Bouvier et al., 2008). Two-stage model ages were estimated according to mean continental crust presuming an average value of 0.015 ($^{176}Lu/^{177}Hf$; Griffin et al., 2000, 2002). However, the depleted-mantle model ages (T_{DM1}) were estimated according to the measured present-day ratio of $^{176}Hf/^{177}Hf$ = 0.28325 (nearly average MORB) and the ratio of $^{176}Lu/^{177}Hf$ = 0.0388.

4. Results

4.1. Petrography

The main mineral assemblage of the medium to coarse-grained Gönen granitoid chiefly comprises K-feldspar (~45%), quartz (~20%), plagioclase (~20%), biotite (~10%), and muscovite (~5%), which show typical holocrystalline texture (Figure 4). The K-feldspar minerals are frequently weathered and occur as mostly subhedral minerals. Sericitic alteration is usually developed within feldspars. Plagioclase, quartz, zircon, and apatite are shown as inclusions within the large K-feldspar crystals. The plagioclase crystals are characterized by polysynthetic twinning and chiefly subhedral shapes. Quartz crystals exhibit typically undulose extinction, some of which are stretched possibly due to local shearing. Biotite crystals are elongated and small crystals, which are partly altered to chlorite. Zircon and apatite crystals form the accessory phases.

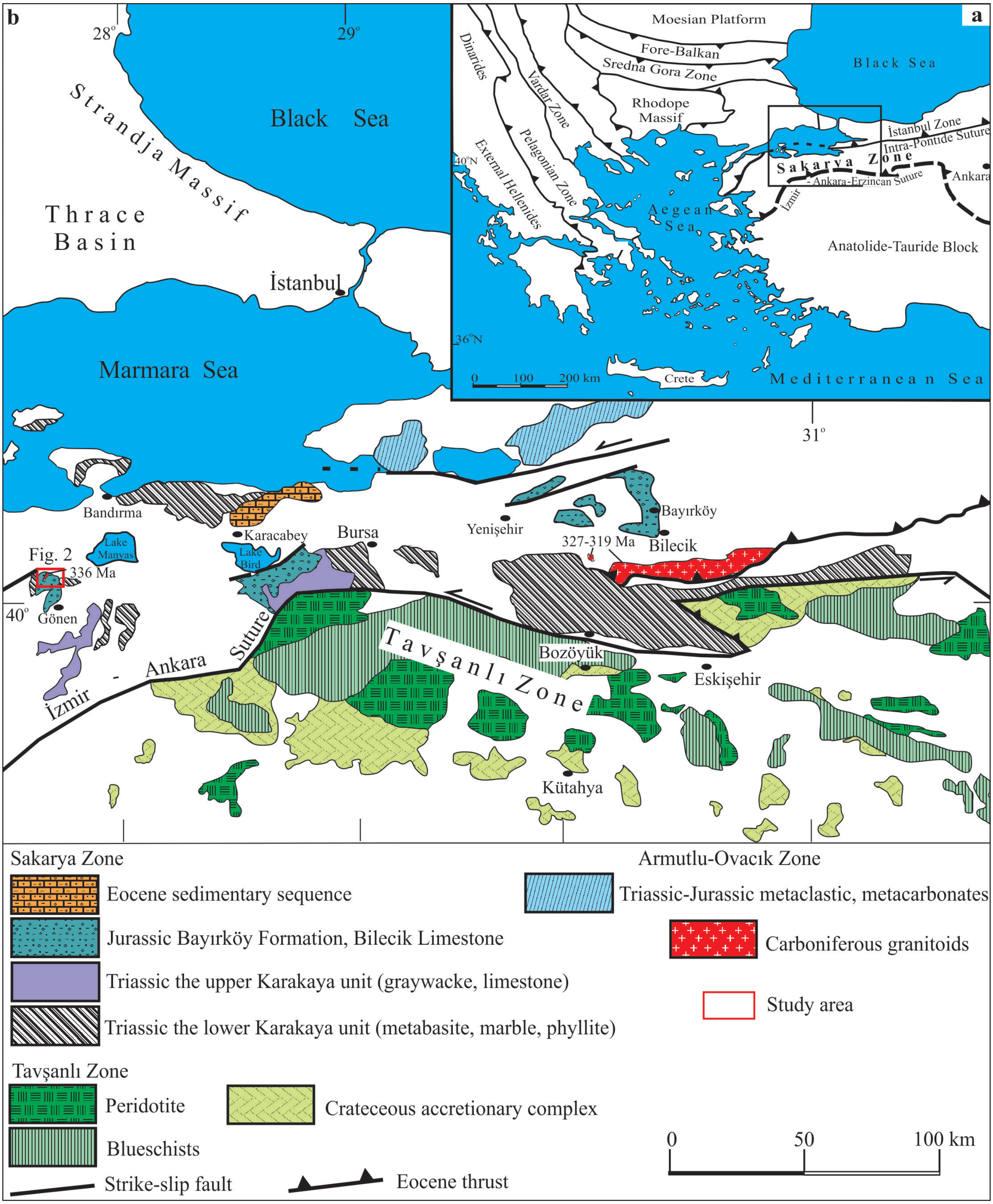

Figure 1. (a) Simplified geotectonic map of the Eastern Mediterranean region (after Okay and Tüysüz, 1999; Meinhold et al., 2010). (b) Geological map of Northwest Turkey showing the outcrops of Carboniferous magmatic rocks (modified from Okay et al., 2006). Isotopic ages are from Ustaömer PA et al. (2012) and this study.

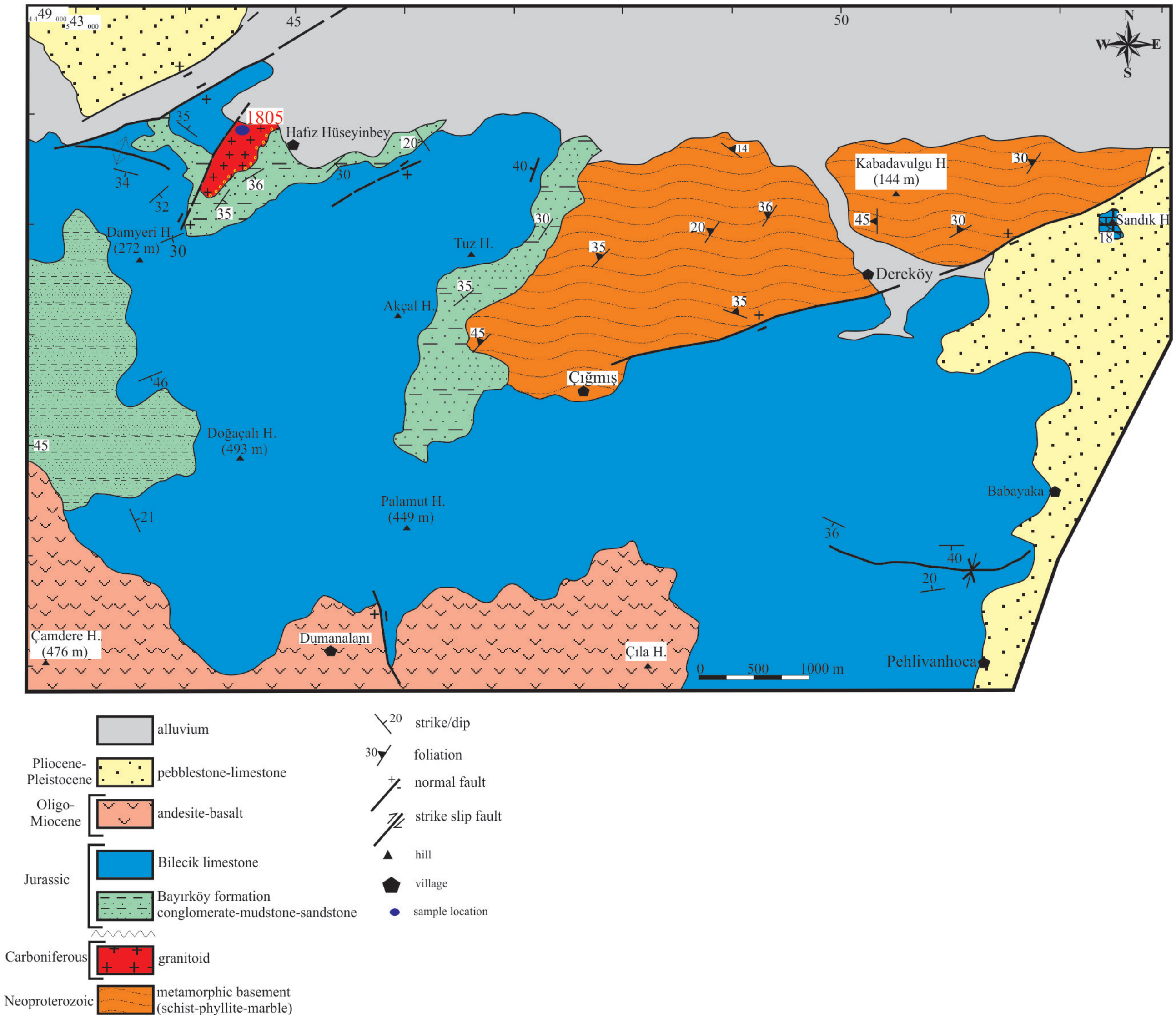

Figure 2. Geological map of the study area together with the location of the dated sample (modified from Yiğitbaş et al., 2010).

4.2. Zircon U-Pb ages

U-Pb zircon isotopic analyses were done on twelve zircon grains from the selected granitoid sample. As shown by CL images (Figures 5a–5g), most of the zircon crystals are colorless, euhedral, and prismatic and have clear oscillatory zoning identical to those from the magmatic rocks. Some zircon grains contain inherited cores (Figures 5e and 5f). The size of zircon grains ranges between 110 µm and 220 µm. The U-Pb isotope data from zircon grains are given in Table 1.

All U-Pb isotopic analyses from twelve zircon grains are concordant within analytical errors (between 90%–110%). $^{206}Pb/^{238}U$ ages of all analyzed zircon grains vary from 345 Ma to 319 Ma (Table 1). $^{206}Pb/^{238}U$ ages of the zircons yielded a concordia age of 336.3 ± 2.9 Ma (Early Carboniferous) with MSWD = 0.054 (Figure 6a). On a Tera–Wasserburg diagram, a similar concordia age of 336.7 ± 2.9 Ma with MSWD = 0.044 was produced (Figure 6b). The concordia age of 336.3 ± 2.9 Ma is regarded as the crystallization time of the Gönen granitoid.

4.3. Zircon Lu-Hf isotopic composition

The same dated zircon crystals in sample 1805 were analyzed for Hf isotopic composition. The initial $^{176}Hf/^{177}Hf$ ratios of all concordant Carboniferous zircon grains (twelve grains) range between 0.282345 and 0.282501 for the Gönen granitoid (Table 2). The $^{176}Hf/^{177}Hf$ ratios are expressed as $\varepsilon_{Hf}(t)$ values according to crystallization ages of each zircon grain for the granitoid. $\varepsilon_{Hf}(t)$ values range from −3.2 to −8.3, which corresponds to 1489–1811 Ma referring to the two-stage Hf model ages.

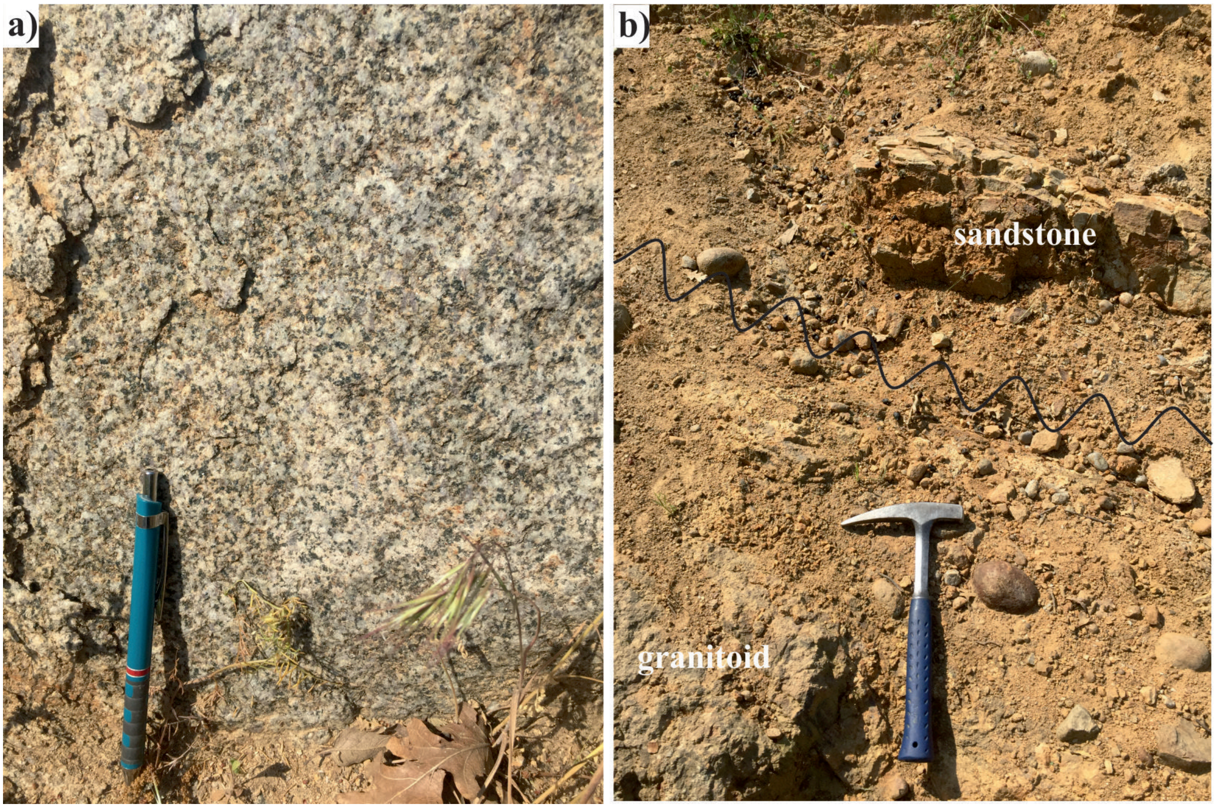

Figure 3. (a) Field photograph of the brown, gray-colored, medium- to coarse-grained Gönen granitoid (west of Hafız Hüseyinbey village); (b) view of contact between the Gönen granitoid and Bayırköy Formation (northwest of Hafız Hüseyinbey village). The contact relationship between them is unconformable.

5. Discussion

5.1. Age of magmatism

The age of the Gönen granitoid was reported to be Oligocene-Early Miocene in a previous study (Akçay et al., 2008). However, this granite is unconformably overlain by clastic rocks of the Jurassic Bayırköy Formation based on field observations, which accurately shows that the Gönen granitoid could not be Oligo-Miocene in age. The zircon U-Pb crystallization age of 336.3 ± 2.9 Ma from the Gönen granitoid sample points to an Early Carboniferous magmatic event. Such Carboniferous Variscan magmatism is common in the Sakarya Zone. The crystallization age of the Söğüt granodiorite ranges from 327 Ma to 319 Ma, which was emplaced into older metamorphic rocks of the Central Sakarya basement (Ustaömer PA et al., 2012). Early to Late Carboniferous granitoids and rhyolites have been well documented in Gümüşhane (Topuz et al., 2010; Karslı et al., 2016), Köse (Dokuz, 2011), Demirözü (Dokuz et al., 2017), and Yusufeli (Ustaömer T et al., 2013) regions in the eastern Sakarya Zone. A similar Carboniferous magmatic event has also been reported from the Biga Peninsula at the westernmost end of the Sakarya Zone. Metavolcanic rocks of the Çamlıca metamorphics yielded zircon U-Pb

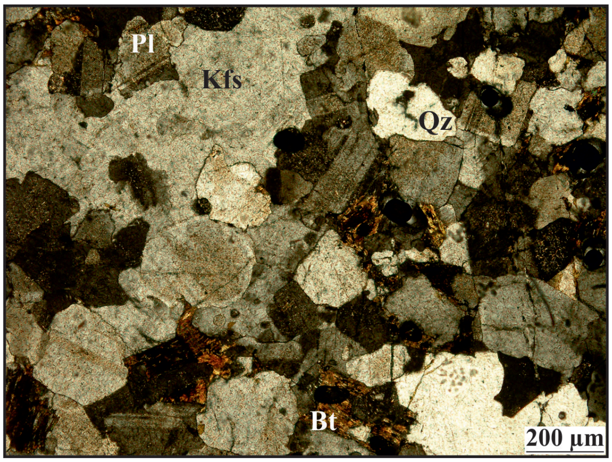

Figure 4. Cross-polarized thin section photomicrograph of the Gönen granitoid (1805). Kfs: K-feldspar, Pl: plagioclase, Qz: quartz, Bt: biotite.

ages of 334 ± 4.8 Ma (Şengün and Koralay, 2017). This Carboniferous magmatism can be attributed to the effect of Variscan orogenic events in the Sakarya Zone (Okay

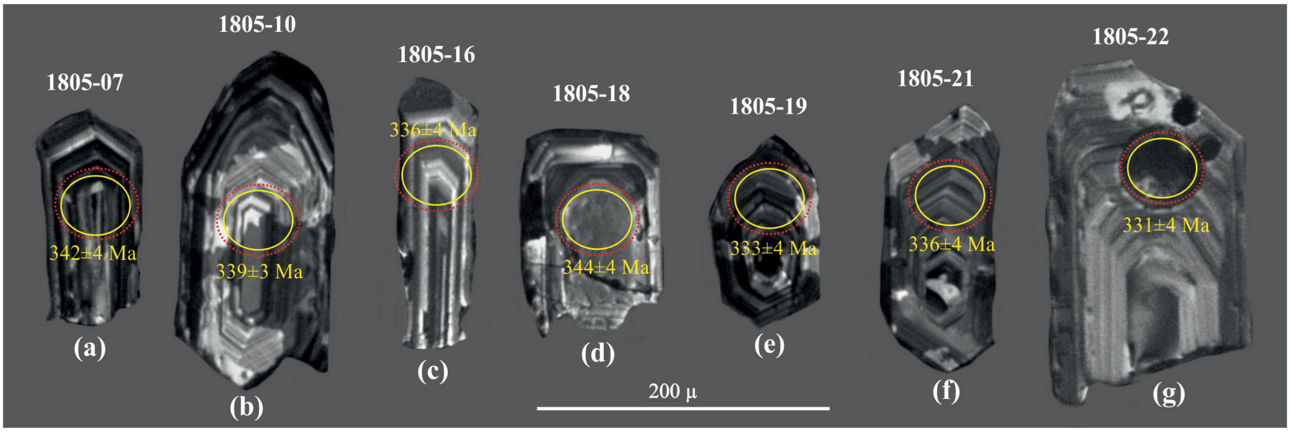

Figure 5. (a–g) Cathodoluminescence (CL) images of representative zircon grains from the Gönen granitoid (sample 1805). The yellow circle and red dashed circle refer to U-Pb and Lu-Hf analytical spots, respectively.

and Nikishin, 2015) and forms a connection between the Variscan orogeny in central Europe and the Uralides of Eastern Europe (Okay et al. 2006). During the Variscan orogeny, continental and oceanic blocks were accreted to the basement of the Sakarya Zone at the southern margin of Laurasia (e.g., Okay et al. 2006; Okay and Nikishin 2015).

The Variscan magmatism can also be traced in the Pelagonian Zone, Balkans, Rhodope Massif, and Cycladic complex (Carrigan et al., 2005; Anders et al., 2007; Schenker et al., 2014; Bonev et al., 2019). Magmatic events in these regions could be attributed to the Variscan orogeny. In the Pelagonian Zone, the Carboniferous basement includes magmatic rocks with an age range of 320 to 307 Ma, which are thought to have formed during subduction events (De Bono, 1998; Vavassis et al., 2000; Stampfli et al., 2013). Carboniferous magmatism is also documented in central Europe in the west (Bonin et al., 1993; Linnemann et al., 2004; Kroner and Romer, 2013) and the Caucasus in the east (Mayringer et al., 2011; Roland et al., 2011). The Variscan orogenic belt in central Europe refers to the continental collision zone between Laurasia to the north and Gondwana to the south (Dewey and Burke, 1974; Matte, 1991). Variscan Massifs in Europe (e.g., the Bohemian Massif, Armorica, Black Forest Massif, French Massif Central, Alpine basements, Moesia) record Carboniferous plutonism and deformation (Linnemann et al., 2004; Carrigan et al., 2005; Ballèvre et al., 2009). During the Early Carboniferous, rocks with monzodioritic to quartz dioritic composition are described in the European Variscides, which were typically emplaced syntectonically between 340 and 330 Ma (Debon and Lemmet, 1999) along major dextral strike–slip faults.

5.2. Magma source

The zircon Lu-Hf composition was used to decipher the magma source, mixing processes, and depleted mantle model ages (T_{DM}) of magmatic rocks (e.g., Griffin et al., 2002). Moreover, when U-Pb ages are combined with corresponding Hf data from the same concordant zircon grains, it gives crucial information about the mantle source from which the protolith of the Gönen granitoid was first separated.

Zircon grains from the Gönen granitoid are characterized by initial $^{177}Hf/^{176}Hf$ isotopic compositions that are below the CHUR (chondritic uniform reservoir) line, which can be ascribed to crustal involvement during magma generation (Figure 7a). Positive $\varepsilon_{Hf}(t)$ values of concordant zircon grains refer to derivation from depleted mantle and formation of juvenile crust (Kroner et al., 2013). However, ancient crust dominated by rocks derived from metasomatized mantle is characterized by negative $\varepsilon_{Hf}(t)$ values (Chen et al., 2008). Zircons from the Gönen granitoid sample have negative $\varepsilon_{Hf}(t)$ values (–3.2 to –8.3), implying involvement of crustal materials during partial melting (Figure 7b). T_{DM} model ages calculated according to the Hf composition of zircon grains vary from 1489 Ma to 1811 Ma, showing that the most ancient crust generation in the Sakarya Zone was ~1100–1500 Ma before the Carboniferous Variscan magmatism. The T_{DM} model ages suggest that Mesoproterozoic/Paleoproterozoic crustal rocks that melted during the Variscan events are common in the Gondwana-derived terranes (Xu et al., 2014; Rapela et al., 2016). Overall, the zircon Hf data presented indicate that the magma source during partial melting was dominated by ancient recycled material.

5.3. Tectonic implications

The Sakarya Zone occurs in the same position as the Pelagonian Zone along the southern margin of Laurasia (Stampfli and Kozur, 2006; Stampfli et al., 2013). This continental ribbon split from the northern margin of Gondwana in the Early Paleozoic and then was dragged northward until it attached to the Laurasian active

Table 1. U-Pb isotopic data of zircon grains from sample 1805.

		Ratios							Age (Ma)						Concordance (%)
Sample	Spot	$^{207}Pb/^{206}Pb$	1SE	$^{207}Pb/^{235}U$	1SE	$^{206}Pb/^{238}U$	1SE	Rho	$^{207}Pb/^{206}Pb$	1σ	$^{207}Pb/^{235}U$	1σ	$^{206}Pb/^{238}U$	1σ	$^{206}Pb/^{238}U$ $^{207}Pb/^{235}U$
1805	1805-01	0.05382	0.00067	0.38832	0.00638	0.052333	0.000559	0.650	363	27	333	5	329	3	98.8
1805	1805-07	0.05283	0.00061	0.39743	0.00649	0.054556	0.000633	0.711	322	25	340	5	342	4	100.6
1805	1805-10	0.05322	0.00062	0.39647	0.00618	0.054029	0.000563	0.668	338	25	339	4	339	3	100
1805	1805-16	0.05311	0.00063	0.39145	0.00632	0.053456	0.000585	0.677	334	26	335	5	336	4	100.3
1805	1805-17	0.05418	0.00063	0.41056	0.00657	0.054959	0.000604	0.687	379	25	349	5	345	4	98.9
1805	1805-18	0.05356	0.00062	0.40493	0.00643	0.054837	0.000597	0.685	352	25	345	5	344	4	99.7
1805	1805-19	0.05243	0.00064	0.38268	0.00666	0.05294	0.000655	0.712	304	27	329	5	333	4	101.2
1805	1805-20	0.05331	0.00063	0.38237	0.00635	0.052659	0.000626	0.725	342	27	321	5	319	4	99.4
1805	1805-22	0.05352	0.00061	0.38889	0.00645	0.052703	0.00063	0.721	351	25	334	5	331	4	99.1
1805	1805-21	0.05280	0.00064	0.38993	0.00683	0.053561	0.000678	0.723	320	26	334	5	336	4	100.6
1805	1805-15	0.05323	0.00064	0.38233	0.00616	0.052094	0.000558	0.665	339	27	329	5	327	3	99.4
1805	1805-14	0.05338	0.00063	0.40392	0.00677	0.054875	0.000655	0.712	345	26	344	5	344	4	100

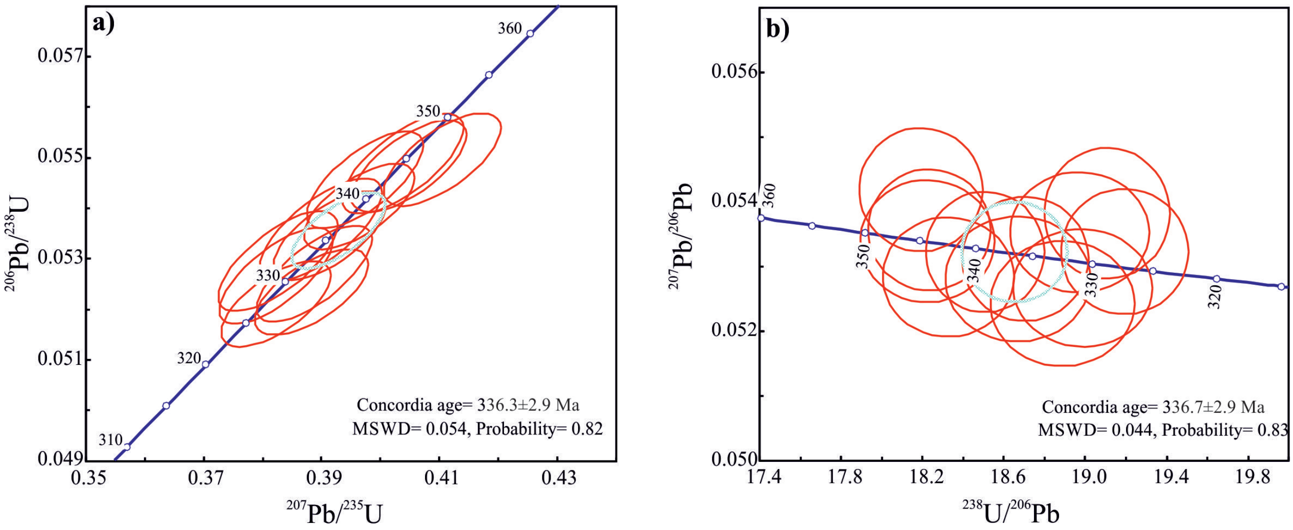

Figure 6. U-Pb diagrams of (a) concordia and (b) Tera–Wasserburg for zircons from dated sample 1805.

Table 2. Hf isotopic data for zircon grains from sample 1805.

Sample	Spot	Age	$^{176}Hf/^{177}Hf$	1SE	$^{178}Hf/^{177}Hf$	1SE	$^{176}Lu/^{177}Hf$	1SE	$^{176}Yb/^{177}Hf$	1SE	$(^{176}Hf/^{177}Hf)t$	εHf(t)	T_{DM1} (Ma)	T_{DM2} (Ma)
1805	1805-01	329	0.282351	0.000012	1.46720	0.00003	0.0012	0.00001	0.0528	0.00034	0.282344	-8.3	1265	1801
1805	1805-07	342	0.282374	0.000010	1.46720	0.00002	0.0026	0.00002	0.1283	0.00060	0.282358	-7.5	1280	1763
1805	1805-10	339	0.282345	0.000010	1.46723	0.00002	0.0014	0.00006	0.0610	0.00310	0.282336	-8.3	1279	1811
1805	1805-16	336	0.282380	0.000006	1.46729	0.00002	0.0012	0.00003	0.0547	0.00068	0.282372	-7.1	1225	1734
1805	1805-17	345	0.282366	0.000012	1.46722	0.00002	0.0028	0.00008	0.1235	0.00310	0.282348	-7.8	1300	1782
1805	1805-18	344	0.282386	0.000011	1.46728	0.00002	0.0035	0.00010	0.1596	0.00470	0.282364	-7.3	1295	1749
1805	1805-19	333	0.282454	0.000009	1.46732	0.00003	0.0014	0.00004	0.0607	0.00210	0.282446	-4.6	1127	1576
1805	1805-20	319	0.282353	0.000009	1.46732	0.00002	0.0016	0.00004	0.0717	0.00120	0.282343	-8.3	1276	1808
1805	1805-22	331	0.282501	0.000013	1.46726	0.00003	0.0024	0.00005	0.1096	0.00290	0.282486	-3.2	1090	1489
1805	1805-21	336	0.282416	0.000012	1.46727	0.00002	0.0040	0.00010	0.1916	0.00380	0.282391	-6.5	1270	1695
1805	1805-15	327	0.282375	0.000013	1.46727	0.00003	0.0013	0.00006	0.0575	0.00240	0.282367	-7.5	1236	1752
1805	1805-14	344	0.282401	0.000018	1.46728	0.00003	0.0034	0.00003	0.1536	0.00150	0.282379	-6.7	1268	1714

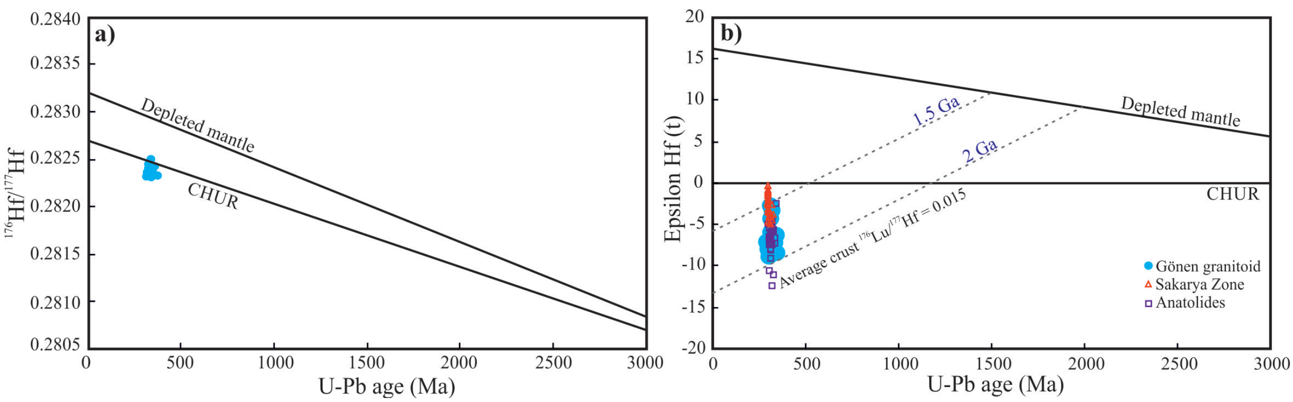

Figure 7. Plot of zircon (a) initial $^{176}Hf/^{177}Hf$ and (b) ε_{Hf} (t) values versus U-Pb ages for the Gönen granitoid. Data from the Sakarya Zone and Anatolides are from Karslı et al. (2016), Ustaömer T et al. (2016), and Ustaömer T et al. (2019), respectively.

continental margin in the Early Carboniferous (Stampfli and Kozur, 2006; von Raumer et al., 2009; Candan et al., 2016). According to a contradictory model by Dokuz et al. (2011), on the other hand, Carboniferous Variscan metamorphism and associated anatexis followed by emplacement of numerous I-type granitoid plutons was due to the collision of a continental ribbon, rifted from the southern margin of Laurasia, with Gondwana to the south. Zircon Lu-Hf systematics of the Gönen Granitoid are consistent with derivation from a continental protolith. Collisional settings appear to be more capable of supplying suitable conditions for the melting of such pure continental materials than subduction zones because of the inevitable contribution of mantle-derived melts.

6. Conclusions

The Gönen granitoid is a small outcrop located in the western Sakarya Zone and unconformably overlain by Jurassic sedimentary rocks. Zircon U-Pb dating produced a concordia age of 336.3 ± 2.9 Ma for the Gönen granitoid. This age refers to the age of crystallization of this granitoid. The Gönen granitoid has negative $\varepsilon_{Hf}(t)$ values varying between –3.2 and –8.3 showing that the parental magma of the granitoid was derived from ancient crust. T_{DM} model ages (1811–1489 Ma) calculated from the Hf composition of zircon grains indicate that the age of recycled crust could be Mesoproterozoic/Paleoproterozoic. The recycling of Mesoproterozoic/Paleoproterozoic crust played a crucial role during the formation of the Gönen granitoid (336.3 ± 2.9 Ma) in the Sakarya Zone. Model ages show that the Carboniferous magmatism evolved from ancient crust, which was possibly extracted from enriched lithospheric mantle in a time interval of 1811 to 1489 Ma. Hf data from zircons demonstrate that a homogeneous and old enriched lithospheric mantle source participated in the formation of the protolith for the Gönen granitoid. Finally, the Carboniferous magmatism involved a collisional event in the early Carboniferous rather than ongoing subduction.

Acknowledgments

This study was supported by the National Postdoctoral Research Scholarship Program (2219) and the Scientific Research Coordination Unit of Çanakkale Onsekiz Mart University under project number of FBA-2017-1319. Constructive reviews by Abdurrahman Dokuz and an anonymous reviewer helped to clarify the picture and considerably improved the manuscript.

References

Akçay AE, Dönmez M, Ilgar A, Duru M, Pehlivan Ş (2008). Bandırma-H19 paftası, Jeoloji Haritası. Ankara, Turkey: MTA Publications (in Turkish).

Anders B, Reischmann T, Kostopoulos D (2007). Zircon geochronology of basement rocks from the Pelagonian Zone, Greece: constraints on the pre-Alpine evolution of the westernmost internal Hellenides. International Journal of Earth Sciences 96: 639-661.

Andersen T, Andersson UB, Graham S, Åberg G, Simonsen SL (2009). Granitic magmatism by melting of juvenile continental crust: new constraints on the source of Palaeoproterozoic granitoids in Fennoscandia from Hf isotopes in zircon. Journal of Geological Society of London 166: 233-24.

Aysal N, Öngen S, Peytcheva I, Keskin M (2012a). Origin and evolution of the Havran Unit, Western Sakarya basement (NW Turkey): new LA-ICP-MS U-Pb dating of the metasedimentary-metagranitic rocks and possible affiliation to Avalonian microcontinent. Geodinamica Acta 25 (3-4): 226-247.

Aysal N, Ustaömer T, Öngen S, Keskin M, Köksal S et al. (2012b). Origin of the Early-Middle Devonian magmatism in the Sakarya Zone, NW Turkey: geochronology, geochemistry and isotope systematics. Journal of Asian Earth Sciences 45: 201-222.

Ballèvre M, Bosse V, Ducassou C, Pitra P (2009). Palaeozoic history of the Armorican Massif: models for the tectonic evolution of the suture zones. Comptes Rendus Geoscience 341:174-201.

Block S, Jessell M, Aillères L, Baratoux L, Bruguier O et al. (2016). Lower crust exhumation during Paleoproterozoic (Eburnean) orogeny, NW Ghana, West African Craton: interplay of coeval contractional deformation and extensional gravitational collapse. Precambrian Research 274: 82-109.

Bonev N, Filipov P, Raicheva R, Moritz R (2019). Timing and tectonic significance of Paleozoic magmatism in the Sakar unit of the Sakar Strandzha Zone, SE Bulgaria. International Geology Review 61 (16): 1957-1979.

Bonin B, Brändlein P, Bussy F, Desmons J, Eggenberger U et al. (1993). Late Variscan magmatic evolution of the Alpine basement. In: von Raumer JF, Neubauer F (editors). The Pre-Mesozoic Geology in the Alps. Berlin, Germany: Springer, pp. 169-199.

Bouvier A, Vervoot JD, Patchett PJ (2008). The Lu–Hf and Sm–Nd isotopic composition of CHUR: constraints from unequilibrated chondrites and implications for the bulk composition of terrestrial planets. Earth and Planetary Science Letters 273: 48-57.

Brown M (2013). Granite: from genesis to emplacement. Geological Society of America Bulletin 125: 1079-1113.

Candan O, Akal C, Koralay OE, Okay AI, Oberhansli R et al. (2016). Carboniferous granites on the northern margin of Gondwana, Anatolide-Tauride Block, Turkey – Evidence for southward subduction of Paleotethys. Tectonophysics 683: 349-366.

Carrigan CW, Mukasa SB, Haydoutov I, Kolcheva K (2005). Age of Variscan magmatism from the Balkan sector of the orogen, central Bulgaria. Lithos 82: 125-147.

Chen JL, Xu XY, Zeng GX, Xiao L, Wang HL et al. (2008). Geochemical characters and LA-ICPMS zircon U–Pb dating constraints on the petrogenesis and tectonic setting of the Shichuan intrusion, east segment of the Central Qilian, NW China. Acta Petrologica Sinica 24: 841-854 (in Chinese with English abstract).

Clemens, JD, Stevens G (2012). What controls chemical variation in granitic magmas? Lithos 134-135: 317-329.

Condie KC, Beyer E, Belousova E, Griffin WL, O'Reilly SY (2005). U-Pb isotopic ages and Hf isotopic composition of single zircons: the search for juvenile Precambrian continental crust. Precambrian Research 139: 42-100.

Debon F, Lemmet M (1999). Evolution of Mg/Fe ratios in late Variscan plutonic rocks from the External Crystalline Massifs of the Alps (France, Italy, Switzerland). Journal of Petrology 40: 1151-1185.

De Bono A (1998). Pelagonian Margins in central Evia island (Greece): Stratigraphy and geodynamic evolution. PhD, University of Lausanne, Lausanne, Switzerland.

Dewey JF, Burke ACK (1973). Tibetan, Variscan, and Precambrian basement reactivation: products of continental collision. Journal of Geology 81 (6): 683-692.

Dokuz A (2011). A slab detachment and delamination model for the generation of Carboniferous high potassium I-type magmatism in the Eastern Pontides, NE Turkey: Köse composite pluton. Gondwana Research 19: 926-944.

Dokuz A, Külekçi E, Aydınçakır E, Kandemir R, Alçiçek MC et al. (2017). Cordierite-bearing strongly peraluminous Cebre Rhyolite from the eastern Sakarya Zone, NE Turkey: constraints on the Variscan Orogeny. Lithos 278-281: 285-302.

Dokuz A, Uysal I, Kaliwoda M, Karslı O, Ottley CJ et al. (2011). Early abyssal- and late SSZ-type vestiges of the Rheic oceanic mantle in the Variscan basement of the Sakarya Zone, NE Turkey: implications for the sense of subduction and opening of the Paleotethys. Lithos 127 (1-2): 176-191.

Elburg M, Andersen T, Bons PD, Simonsen SL, Weisheit A (2013). New constraints on Phanerozoic magmatic and hydrothermal events in the Mt Painter Province, South Australia. Gondwana Research 24: 700-712.

Erdoğan B, Akay E, Hasözbek A, Satır M, Siebel W (2013). Stratigraphy and tectonic evolution of the Kazdağ Masif (NW Anatolia) based on field studies and radiometric ages. International Geology Review 55: 2060-2082.

Gao P, Zheng YF, Zhao ZF (2017). Triassic granites in South China: A geochemical perspective on their characteristics, petrogenesis, and tectonic significance. Earth-Science Reviews 173: 266-294.

Gill R (2010). Igneous Rocks and Processes: A Practical Guide. Oxford, UK: Wiley-Blackwell.

Griffin WL, Pearson NJ, Belousova E, Jackson SE, van Achterbergh E et al. (2000). The Hf isotope composition of cratonic mantle: LA-MCICPMS analysis of zircon metacrysts in kimberlites: Geochimica et Cosmochimica Acta 64: 133-147.

Griffin WL, Wang X, Jackson SE, Pearson NJ, O'Reilly SY et al. (2002). Zircon chemistry and magma mixing, SE China: In-situ analysis of Hf isotopes. Tonglu and Pingtan igneous complexes. Lithos 61: 237-269.

Hawkesworth CJ, Kemp AIS (2006). Evolution of the continental crust. Nature 443: 811-817.

Heinonen AP, Andersen T, Rämö OT (2010). Re-evaluation of Rapakivi petrogenesis: source constraints from the Hf isotope composition of zircon in the Rapakivi Granites and associated mafic rocks of Southern Finland. Journal of Petrology 51: 1687-1709.

Jackson SE, Pearson NJ, Griffin WL, Belousova EA (2004). The application of laser ablation-inductively coupled plasma-mass spectrometry to in situ U–Pb zircon geochronology. Chemical Geology 211: 47-69.

Karslı O, Dokuz A, Kandemir R (2016). Subduction-related Late Carboniferous to Early Permian Magmatism in the Eastern Pontides, the Camlik and Casurluk plutons: Insights from geochemistry, whole-rock Sr–Nd and in situ zircon Lu–Hf isotopes, and U–Pb geochronology. Lithos 266-267: 98-114.

Kaygusuz A, Arslan M, Sipahi F, Temizel İ (2016). U–Pb zircon chronology and petrogenesis of Carboniferous plutons in the northern part of the Eastern Pontides, NE Turkey: constraints for Paleozoic magmatism and geodynamic evolution. Gondwana Research 39: 327-346.

Kemp AIS, Hawkesworth CJ, Foster GL, Paterson BA, Woodhead JD et al. (2007). Magmatic and crustal differentiation history of granitic rocks from Hf-O isotopes in zircon. Science 315: 980-983.

Kroner A, Kovach V, Belousova E, Hegner E, Armstrong R et al. (2014). Reassessment of continental growth during the accretionary history of the Central Asian Orogenic Belt. Gondwana Research 25: 103-125.

Kroner U, Romer RL (2013). Two plates-many subduction zones: the Variscan orogeny reconsidered. Gondwana Research 24: 298-329.

Lauri LS, Andersen T, Hölttä P, Huhma H, Graham S (2011). Evolution of the Archaean Karelian province in the Fennoscandian Shield in the light of U–Pb zircon ages and Sm–Nd and Lu–Hf isotope systematics. Journal of Geological Society of London 168: 201-218.

Linnemann U, McNaughton NJ, Romer RL, Gehmlich M, Drost K et al. (2004). West African provenance for Saxo-Thuringia (Bohemian Massif): did Armorica ever leave pre-Pangean Gondwana? U-Pb-SHRIMP zircon evidence and the Nd-isotopic record. International Journal of Earth Sciences 93: 683-705.

Lu YH, Zhao ZF, Zheng YF (2017). Geochemical constraints on the nature of magma sources for Triassic granitoids from South Qinling in central China. Lithos 284-285: 30-49.

Ludwig KR (2012). User's Manual for Isoplot 3.75: A Geochronological Toolkit for Microsoft Excel. Berkeley, CA, USA: Berkeley Geochronology Center.

Matte P (1991). Accretionary history of the Variscan belt in western Europe. Tectonophysics 43: 109-125.

Mayringer F, Treloar PJ, Gerdes A, Finger F, Shengelia D (2011). New age data from the Dzirula Massif, Georgia: implications for the evolution of the Caucasian Variscides. American Journal of Science 311: 404-441.

Meinhold G, Kostopoulos D, Frei D, Himmerkus F, Reischmann T (2010). U-Pb LA-SF ICP-MS zircon geochronology of the Serbo-Macedonian Massif, Greece: palaeotectonic constraints for Gondwana-derived terranes in the Eastern Mediterranean. International Journal of Earth Sciences 99: 813-832.

Okay Aİ, Göncüoğlu MC (2004). The Karakaya Complex: A review of data and concepts. Turkish Journal of Earth Sciences 13: 77-95.

Okay AI, Nikishin AM (2015). Tectonic evolution of the southern margin of Laurasia in the Black Sea region. International Geology Review 57 (5-8): 1051-1076.

Okay AI, Satır M, Maluski H, Siyako M, Monie P et al. (1996). Paleo and Neotethyan events in northwest Turkey. In: Yin A, Harrison M (editors). Tectonics of Asia. Cambridge, UK: Cambridge University Press, pp. 420-441.

Okay AI, Satir M, Siebel W (2006). Pre-Alpide and Mesozoic orogenic events in the Eastern Mediterranean region. Journal of Geological Society of London Special Publications 32: 389-405.

Okay AI, Siyako M, Bürkan KA (1991). Geology and tectonic evolution of the Biga Peninsula. Bulletin of the Technical University of Istanbul 44: 191-255.

Okay AI, Tüysüz O (1999). Tethyan sutures of northern Turkey. In: Durand B, Jolivet L, Horváth F, Séranne M (editors). The Mediterranean Basins: Tertiary Extension within the Alpine Orogen. London, UK: Geological Society of London Special Publications, pp. 475-515.

Pitcher WS (1997). The Nature and Origin of Granite. 2nd edition. London, UK: Chapman and Hall.

Rapela CW, Verdecchia SO, Casquet C, Pankhurst RJ, Baldo EG et al. (2016). Identifying Laurentian and SW Gondwana sources in the Neoproterozoic to Early Paleozoic metasedimentary rocks of the Sierras Pampeanas: paleogeographic and tectonic implications. Gondwana Research 32: 193-212.

Rolland Y, Sosson M, Adamia S, Sadradze N (2011). Prolonged Variscan to Alpine history of an active Eurasian margin (Georgia, Armenia) revealed by $^{40}Ar/^{39}Ar$ dating. Gondwana Research 20: 798-815.

Schenker FL, Burg JP, Kostopoulos D, Moulas E, Larionov A et al. (2014). From Mesoproterozoic magmatism to collisional Cretaceous anatexis: tectonomagmatic history of the Pelagonian Zone, Greece. Tectonics 33: 1552-1576.

Şengün F, Koralay OE (2017). Early Variscan magmatism along the southern margin of Laurasia: Geochemical and geochronological evidence from the Biga Peninsula, NW Turkey. International Journal of Earth Sciences 106: 811-826.

Söderlund U, Patchett PJ, Vervoort JD, Isachsen CE (2004). The ^{176}Lu decay constant determined by Lu-Hf and U-Pb isotope systematics of Precambrian mafic intrusions. Earth and Planetary Science Letters 219: 311-324.

Stampfli GM, Borel GD (2002). A plate tectonic model fort the Paleozoic and Mesozoic constrained by dynamic plate boundaries and restored synthetic oceanic isochrones. Earth and Planetary Science Letters 196: 17-33.

Stampfli GM, Hochard C, Verard C, Wilhem C, von Raumer J (2013). The formation of Pangea. Tectonophysics 593: 1-19.

Stampfli GM, Kozur H (2006). Europe from the Variscan to the Alpine cycles. In: Gee DG, Stephenson R (editor) European lithosphere dynamics. Geological Society of London Memoirs 32: 57-82.

Sunal G (2012). Devonian magmatism in the western Sakarya Zone, Karacabey Region, NW Turkey. Geodinamica Acta 25: 183-201.

Topuz G, Altherr R, Kalt A, Satır M, Werner O et al. (2004). Aluminous granulites from the Pulur complex, NE Turkey: a case of partial melting, efficient melt extraction and crystallization. Lithos, 72: 183-207.

Topuz G, Altherr R, Schwarz WH, Dokuz A, Meyer H (2007). Variscan amphibolite-facies rocks from the Kurtoğlu Metamorphic Complex (Gümüşhane Area, Eastern Pontides, Turkey). International Journal of Earth Sciences 96: 861-873.

Topuz G, Altherr R, Siebel W, Schwarz WH, Zack T et al. (2010). Carboniferous high-potassium I-type granitoid magmatism in the Eastern Pontides: the Gümüşhane pluton (NE Turkey). Lithos 116: 92-110.

Ustaömer PA, Ustaömer T, Robertson AHF (2012). Ion Probe U-Pb Dating of the Central Sakarya Basement: a peri-Gondwana Terrane Intruded by late Lower Carboniferous Subduction/Collision-related Granitic Rocks. Turkish Journal of Earth Sciences 21: 905-932.

Ustaömer T, Robertson AHR, Ustaömer PA, Gerdes A, Peytcheva I (2013). Constraints on Variscan and Cimmerian magmatism and metamorphism in the Pontides (Yusufeli-Artvin area), NE Turkey from U-Pb dating and granite geochemistry. In: Robertson AHF, Parlak O, Ünlügenç UC (editors). Geological Development of Anatolia and the Easternmost Mediterranean Region. London, UK: Geological Society of London, pp. 49-74.

Ustaömer T, Ustaömer PA, Robertson AHR, Gerdes A (2019). U-Pb-Hf isotopic data from detrital zircons in late Carboniferous and Mid-Late Triassic sandstones, and also Carboniferous granites from the Tauride and Anatolide continental units in S Turkey: implications for Tethyan paleogeography. International Geology Review (in press). doi: 10.1080/00206814.2019.1636415

Vavassis I, De Bono A, Stampfli G, Giorgis D, Valloton A et al. (2000). U-Pb and Ar-Ar geochronological data from the Pelagonian Basement in Evia (Greece). Geodynamic implications for the evolution of Paleotethys. Swiss Bulletin of Mineralogy and Petrology 80: 21-43.

Von Raumer JF, Stampfli GM, Bussy F (2009). The Variscan evolution in the External massifs of the Alps and place in their Variscan framework. Comptes Rendus Geoscience 341: 239-252.

Wiedenbeck M, Alle P, Corfu F, Griffin WL, Meier M et al. (1995). Three natural zircon standards for U–Th–Pb, Lu–Hf, trace element and REE analyses. Geostandards Newsletter 19: 1-23.

Woodhead JD, Hergt JM (2005). Preliminary appraisal of seven natural zircon reference materials for in situ Hf isotope determination. Geostandards and Geoanalytical Research 29: 183-195.

Xu Y, Cawood PA, Du Y, Zhong Z, Hughes NC (2014). Terminal suturing of Gondwana along the southern margin of South China Craton: evidence from detrital zircon U-Pb ages and Hf isotopes in Cambrian and Ordovician strata, Hainan Island. Tectonics 33: 2490-2504.

Yiğitbaş E, Tunç İO, Şengün F (2010). Some major geological problems and tectono-stratigraphic features of the Pre-Cenezoic units in the Biga Peninsula. In: Karadeniz Technical University Department of Geological Engineering 45th Anniversary Symposium, Trabzon, Turkey, pp. 141-143.

Zeh A, Jaguin J, Poujol M, Boulvais P, Block S et al. (2013). Juvenile crust formation in the northeastern Kaapvaal Craton at 2.97 Ga—Implications for Archean terrane accretion, and the source of the Pietersburg gold. Precambrian Research 233: 20-43.